J. Chem. Sci., Vol. 122, No. 2, March 2010, pp. 259–269.

A comparative study of the spectroscopic features of the low-lying electronic states of H_2F^+ and H_2Cl^+ ions

ANJAN CHATTOPADHYAY

Chemistry Group, Birla Institute of Technology and Science (BITS), Pilani – Goa Campus, Goa 403 726
e-mail: anjan_chattopadhyay@yahoo.com; anjan@bits-goa.ac.in

MS received 30 April 2009; revised 30 August 2009; accepted 23 December 2009

Abstract. Configuration interaction studies of H_2F^+ and H_2Cl^+ ions, using 6-311G (3*d*, 3*p*) basis sets, have revealed several interesting differences in their spectral behaviour. Both of them are having bent ground state ($^1A_1$) equilibrium geometries, but there is a huge difference (~1·93 eV) between their energy barrier to linearity. Their first two excited states are found to be linear $^3\Pi_u$ and $^1\Pi_u$ states, correlating to $^3B_1/^3A_1$ and $^1B_1/^1A_1$ Renner–Teller pairs, respectively, in the C_{2v} symmetry. Considering only the allowed singlet–singlet transitions at the ground state equilibrium geometry, the lowest energy transitions found to have transition moment values of 0·65 D and 0·48 D for $H_2F^+$and H_2Cl^+, respectively, appearing in the far UV region. Conical intersections take place during the symmetrical stretching of two H–Cl bonds in the chloronium ion for the first two pairs of excited states ($1^3A_2/1^3B_1$ and $1^1A_2/1^1B_1$) in the C_{2v} symmetry. This intersection may initiate pre-dissociation from the upper bound adiabatic $^1A''$ state to the lower repulsive $^1A''$ state in the C_s symmetry. Fluoronium ion is expected to dissociate via a single electronic state due to the absence of such intersection.

Keywords. Configuration interaction; electronic states; transition moment.

1. Introduction

Over the past several decades, molecular ions have gained considerable attention due to their importance in various fields, such as, organic reactions, interstellar space, planetary atmospheres, electrical discharges, and so on. This present work highlights the spectroscopic properties of the electronic states of two important halonium ions, those are yet to be revealed experimentally. Existence of fluoronium ion was first proposed by Hanztsch[1,2] in non-aqueous hydrofluoric acid system. In solution chemistry its importance is well known as a superacid. This isoelectronic species of water is also important due to its possible existence in the interstellar medium. Couzi and co-workers[3] first identified the infrared spectrum of this ion. Schäfer and Saykally[4,5] studied the velocity modulation infrared laser spectroscopy of the ν_1 and ν_3 bands. Several other experimental work[6,7] along with different level of theoretical calculations,[8–20] starting from self-consistent-field (SCF) to multiconfiguration self-consistent-field configuration interaction (MCSCF-CI) methods were investigated by different groups. Studies on *ab initio* rotation–vibration energies[21] and optimized geometries, using quadratic configuration interaction method at second-order Møller–Plesset level[22] were carried out in the last decade. Chloronium ion is known to be an important intermediate in ion–molecule reactions. This is one of the chlorine-bearing species in the interstellar clouds.[23,24] This ion has been detected in the gas phase by infra-red diode laser spectroscopy with magnetic field modulation. A hollow cathode discharge in H_2, He and HCl mixture generates this ion. Blake *et al*[25] estimated the fractional abundances of different chlorine-bearing molecular species. H_2Cl^+ is one of the most important chlorine containing molecules in space and it is also a major molecular ion giving HCl. Infra-red spectrum of this ion was first observed in the laboratory by Kawaguchi and Hirota.[26] They studied the ν_2 band with infra-red diode laser spectroscopy and derived r_0 structure from the observed rotational constants. Gas-phase spectra of the ν_1 and ν_3 bands were reported[27] with a difference-frequency laser spectrometer between 2525 and 2755 cm^{-1}. Saito and co-workers[28] have studied rotational frequencies and determined the rotational constants of this ion. They observed four rotational transitions in the frequency region of 270–

500 GHz by using a source modulated microwave spectrometer combined with a hollow cathode free space cell. Rotational spectrum of H_2Cl^+ was also investigated[29] in the region of 180–550 GHz with a source modulated submillimeter–wave spectrometer. Theoretical studies[30] were first attempted at STO-3G and MINDO/3 level. De Frees *et al*[31] calculated vibrational frequencies at the Hartree–Fock (HF/6-31G*) and second-order Møller–Plesset (MP2/6-31G*) perturbation level of theory. Botschwina[32,33] has employed the coupled electron pair approximation (CEPA) calculations to obtain structure parameters and vibrational frequencies of this ion. Geometries and energies of the singlet and triplet states have been studied at the unrestricted Hartree–Fock (UHF/6-31G*) level.[20] Gaussian-2 theoretical procedure (G2 theory), based on *ab initio* molecular orbital theory was used by Curtiss *et al*[34] to calculate the molecular energy of this ion. Studies at SCF/6-31G**, MP2 (full)/6-31G** and MP2 (full)/TZP levels for the geometrical parameters of this ion have also been reported.[22] Multireference configuration interaction (MRCI) based approach[35] on the low-lying states and methods employing diatomics-in–molecule model,[36,37] to study the $^1A'$ potential energy surfaces, are few more examples of significant work on this molecular ion in the last decade.

In this present work, spectroscopic parameters for low-lying singlet and triplet electronic states are calculated for the two above mentioned halonium ions, using *ab initio* based theoretical methods. Various properties of the ground state and excited states, such as, equilibrium geometries, dominating configurations, bending potentials, dipole moments are reported from configuration interaction (CI) studies. Symmetrical stretching and bending potentials are studied, mainly to highlight the difference in their behaviour appearing due to the intersections of the excited states in the C_{2v} symmetry and consequently their dissociations during the asymmetric pulling of one bond. The reported transition moments and oscillator strengths corresponding to the electronic transitions from the ground state to excited singlet states at the ground state equilibrium geometry could be very useful for the experimentalists working in the far ultraviolet region spectroscopy.

2. Computational details

GAMESS program package[38] has been used for the calculations in this work. 6-311G basis sets with three d polarization functions for the heavier atoms and three *p* polarization functions for the hydrogen atoms have been employed for all calculations. This gives a total of 55 basis functions for H_2F^+ ion and 63 basis functions for H_2Cl^+ ion. Both of them are having similar ground state symmetry ($^1A_1$). In the first step, self-consistent molecular orbital (SCF-MO) calculations have been carried out for their ground states in the C_{2v} symmetry. These SCF-MOs are used for the CI calculations in the next steps. The 2 core electrons of $H_2F^+$are kept frozen in the $1a_1$ MO while for H_2Cl^+, the 10 core electrons are kept frozen in the doubly occupied molecular orbitals ($1a_1$, $2a_1$, $3a_1$, $1b_2$ and $1b_1$). In each case, outer 8 electrons are treated for the CI calculations. For the configuration interaction studies, the Ames Laboratory determinant full (ALDET) CI[39] has been employed throughout this work along with the Graphical Unitary Group Approach (GUGA) CI,[40,41] in some cases. The latter one is mainly used for the transition moment calculations. The Ames Laboratory determinant full CI code was written by Joe Ivanic and Klaus Ruedenberg. ALDET is a full CI within the chosen active space. In GAMESS input file, $CIDET group describes the determinants to be used in a full CI wavefunction. In this present work, for both fluoronium and chloronium ions, calculations have been performed with 8 active electrons (NELS = 8) in 10 active orbitals (NACT = 10), which generate 44100 determinants, in each case. These determinants contain different spin states (S = 0, 1, 2, 3, 4), in contrast to configuration state functions. These CI states include all space symmetries along with the mentioned spin symmetries. The GUGA CI is based on Brooks and Schaefer's[40,41] unitary group program which was modified to run within GAMESS, using a Davidson eigenvector method[42] written by Steve Elbert.[43] Graphical Unitary Group Approach (GUGA) specifies configurations using the Distinct Row Table (DRT) by the $CIDRT group in GAMESS. This DRT defines the Hamiltonian matrix by means of loop-driven algorithm. For H_2F^+ and H_2Cl^+, in the singlet state calculations using restricted Hartree–Fock (RHF) method, 8 valence electrons are kept doubly occupied in 4 orbitals (NDOC = 4) inside the $CIDRT group in the input file. These electrons are excited to the virtual orbitals and the excitation level is selected to be 2 (EXCIT = 2), which gives rise to singles and doubles CI. In each case, the Distinct Row Table is found to have 212 rows and number of configuration

state functions (CSF) generated are 20301. In case of GUGA based triplet state calculations using restricted open-shell Hartree–Fock (ROHF) method, 6 valence electrons are kept doubly occupied in 3 orbitals (NDOC = 3) while 2 alpha spin singly occupied MOs contain 2 electrons (NALP = 2) in the input file. The Distinct Row Table contains 227 rows and number of generated CSF's are 175185. GUGA based multiconfiguration self-consistent-field (MCSCF)[44–50] calculations are also employed to determine geometries of some triplet states. Optimization of the ground state along with few excited singlet and triplet state geometries have been carried out at the CI level in the C_{2V} symmetry. For H_2F^+, first few singlet and triplet roots are studied during the symmetrical stretching of the H–F bonds, starting from a bond distance of 0·5 Å to 2·5 Å and keeping the bond angle fixed at 112°. Similarly, symmetrical stretching of the H–Cl bonds of H_2Cl^+ ion are carried out between 1 Å and 3·5 Å, at a fixed bond angle of 93·9°. In the next stage of calculation these singlet and triplet states are studied varying the bond angles up to 180° and fixing the bond lengths at 0·96 Å and 1·31 Å, for fluoronium and chloronium ions, respectively. Keeping the bond angle and one bond distance fixed at their respective ground state equilibrium values, the other bond distance is varied and the low-lying A′ and A″ states are studied in C_s symmetry. ALDET-CI method has been employed for calculations of all the above mentioned stretching and bending potentials.

Dipole moment values are reported in this work with respect to the center of mass. Radiative transition moments and oscillator strengths[51–53] are calculated from the GAMESS package for electronic transitions between the ground state and some low-lying excited singlet states at the ground-state equilibrium geometry, using the GUGA-CI wavefunctions.

3. Results and discussion

Molecular orbitals generated from the Hartree–Fock calculations are used as the basis for the CI calculations. It is already stated that geometry optimizations of the singlet and triplet states are carried out at the CI level in the C_{2V} symmetry. It should be mentioned here that there might be few more low-lying singlet and triplet states other than the reported ones, arising out from the unsymmetrical geometries (H–X–H and/or H–H–X, where X = F, Cl) of these two halonium ions. Such states are not reported in this work. The present study deals with the symmetrical stretching and bending of the low-lying states. In C_s symmetry, keeping one bond length and bond angle fixed at the ground state equilibrium geometry values, stretching of the other bond is studied to find the low-lying dissociation channels of the bent structures.

3.1 H_2F^+

Equilibrium bond angle and bond distance of the ground state (X^1A_1) are found to be at 112° and 0·96 Å, respectively, from the ALDET-CI level of calculations. GUGA-CI predicted results are very close to these values. The experimentally observed values (table 1) are in good agreement with the calculated ones. The ground state is dominated by a large contribution (99%) from the $2a_1^2 1b_2^2 3a_1^2 1b_1^2$ configuration at the equilibrium geometry. The $2a_1$ MO has purely *s* orbital character of the fluorine atom while the next few high-lying molecular orbitals involve *p* orbitals of the fluorine atom, such as, $2p_y$ AO generates $1b_2$ MO and $2p_z$ AO generates $3a_1$ MO. Both of them have binding character. The $1b_1$ molecular orbital, localized on the fluorine atom, has non-bonding character as $2p_x$ orbital has no overlap with the H atoms. The barrier to linearity for the ground state is 0·84 eV (table 1). In the $D_{\infty h}$ symmetry, this bent state correlates to a linear $^1\Sigma_g^+$ state with a dominating configuration of $\sigma_g^2\sigma_u^2\pi_u^4$.

Studies of the excited states reveal that triplet states are lower in energy than singlet states. Varying the two H–F bond distances symmetrically (figure 1a), the first two excited electronic states are found to be of $^3B_1$ and $^3A_2$ symmetry. Geometry optimization result shows that the lowest energy triplet state (1^3B_1) is actually a linear one ($^3\Pi_u$) with equilibrium bond distance at 1·485 Å. MCSCF result is found to be little lower (~0·02 Å) than the ALDET-CI predicted value (Table 1). This $^3\Pi_u$ state has another component (1^3A_1) in the C_{2v} symmetry. A linear/linear Renner–Teller effect couples the electronic angular momentum to the vibrational angular momentum. This coupling causes breakdown of the Born–Oppenheimer approximation, since the electronic and vibrational motions can no longer be treated independently. The second excited triplet state (1^3A_2) is found to be bent with a large contribution from $2a_1^2 1b_1 1b_2^2 3a_1^2 4a_1^2 2b_2$ configuration. The geometry of the first excited singlet state (1^1B_1) is

Table 1. Spectroscopic parameters of ground state and some low-lying excited states of H_2F^+.

States in C_{2v} symmetry	Level of study	Equilibrium geometry: Bond length (H–Cl) (Å)	Equilibrium geometry: Bond angle (H–Cl–H) (deg)	Most dominant configuration	Energy barrier to linearity (eV)	Dipole moment at equilibrium geometry (Debye)
X^1A_1	**ALDET-CI**	0·960	112·0	$2a_1^2 1b_2^2 3a_1^2 1b_1^2$	0·84	2·51
	GUGA-CI	0·955	112·5			2·59[g]
	SCF[a]	0·945	114·8			
	CI (SD)[a]	0·961	112·7			
	SCF [b]	0·950	114·7			
	CI[c]	0·963	112·1			
	SCF (UHF)[d]	0·962	114·0			
	Exptl.[e,f]	0·968	113·9			
$^3B_1$ ($^3\Pi_u$ at equilibrium)	**MCSCF**	1·462	180	$2a_1^2 1b_2^2 3a_1^2 1b_1 4a_1$ ($\sigma_g^2\sigma_u^2\pi_u^3\sigma_g$ at equilibrium geometry)	0·00	0·00
	ALDET-CI	1·485	180			
	SCF (UHF)[d]	1·462	180			
$^3A_1$ ($^3\Pi_u$ at equilibrium)	**ALDET-CI**	1·485	180	$2a_1^2 1b_2^2 1b_1^2 3a_1 4a_1$ ($\sigma_g^2\sigma_u^2\pi_u^3\sigma_g$ at equilibrium geometry)	0·00	0·00
	SCF (UHF)[d]	1·462	180			
$^1B_1$ ($^1\Pi_u$ at equilibrium)	**ALDET-CI**	1·472	180	$2a_1^2 1b_2^2 3a_1^2 1b_1 4a_1$ ($\sigma_g^2\sigma_u^2\pi_u^3\sigma_g$ at equilibrium geometry)	0·00	0·00
2^1A_1 ($^1\Pi_u$ at equilibrium)	**ALDET-CI**	1·472	180	$2a_1^2 1b_2^2 3a_1 1b_1^2 4a_1$ ($\sigma_g^2\sigma_u^2\pi_u^3\sigma_g$ at equilibrium geometry)	0·00	0·00
$^3A_2$	**ALDET-CI**	1·800	95·0	$2a_2^2 1b_1 1b_2^2 3a_1^2 4a_1^2 2b_2$	1·41	3·24
	GUGA-CI (ROHF)	1·700	98·0			

[a][7], [b][10], [c][17], [d][20], [e][4], [f][5], [g][21]

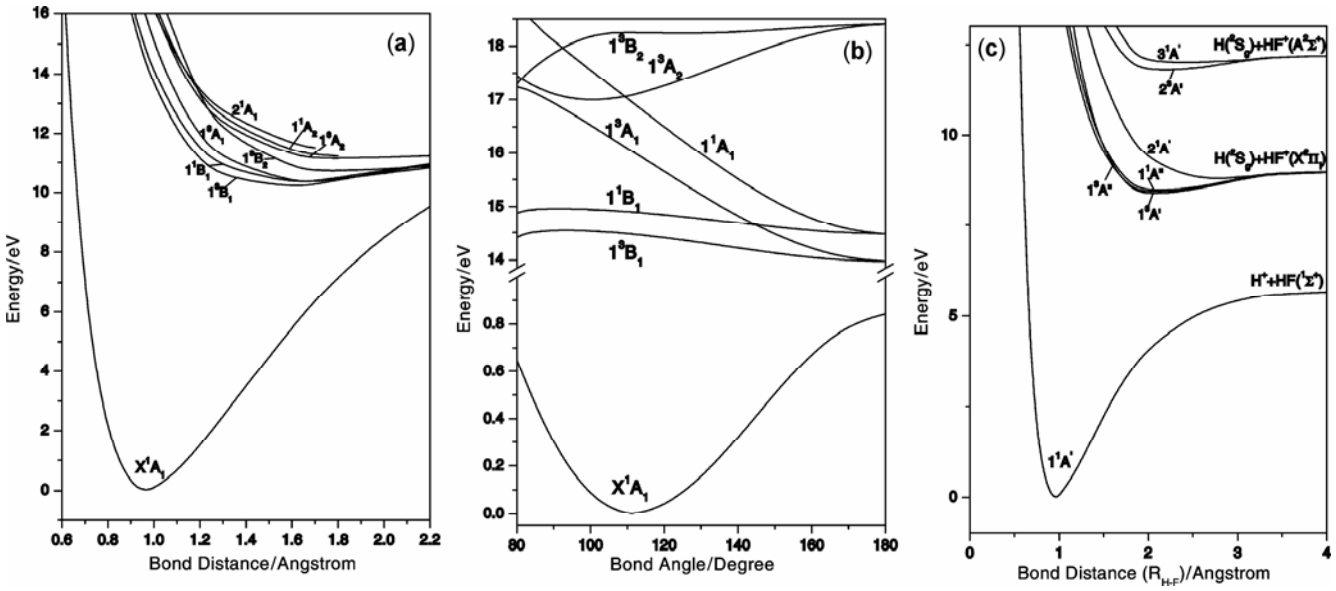

Figure 1. (**a**) One-dimensional potential energy curves of low-lying electronic states during the symmetrical stretching of H–F bonds at the ground-state equilibrium bond angle (112°). (**b**) Bending potential energy curves of the ground state and low-lying excited states of H_2F^+ at R_{H-F} = 0·96 Å. (**c**) Potential energy curves of low-lying electronic states of H_2F^+ during asymmetrical stretching of one H–F bond (the other H–F bond distance is kept fixed to 0·96 Å and bond angle is fixed at 112°).

similar to its triplet counterpart with a small difference in the equilibrium bond distance. In the linear geometry ($^1\Pi_u$), this state is dominated by $\sigma_g^2\sigma_u^2\pi_u^3\sigma_g$ configuration. The second $^1A_1$ state is the other Renner–Teller component of this linear state when $D_{\infty h}$ symmetry changes to C_{2v} symmetry. Energy of the next singlet state (1^1A_2) is very high. Geometry optimization of this state and the next few excited states, such as, 1^3B_2 and 1^1B_2 are not attempted. Bending potential energy curves of the above mentioned states are also studied keeping H–F bond lengths fixed at 0·96 Å (figure 1b).

In C_s symmetry, A′ states correspond to the A_1 states and two A″ states correlate to the B_1 and A_2 states in the C_{2v} symmetry. One H–F bond length is kept fixed at 0·96 Å and bond angle at 112°, while the other H–F bond distance is varied. As shown in Figure 1c, the lowest energy state ($1^1A'$) correlates to the $H^+ + HF$ ($^1\Sigma^+$) dissociation asymptote. The other two lower energy states ($1^3A''$ and $1^1A''$) are found to be very weakly bound. The first $^3A'$ curve is also having a similar behaviour. A strongly repulsive nature is observed for the $2^1A'$ state. All these states dissociate into H (^2S_g) and $HF^+(X^2\Pi_i)$. The next two A′ states with singlet and triplet symmetries correspond to a very high-energy dissociation limit, $H(^2S_g) + HF^+(A^2\Sigma^+)$. The energy gap between second and third dissociation asymptotes is found to be 3·1 eV which is very close to the experimentally obtained value.[54,55] Energies of the first two dissociation asymptotes obtained during the asymmetrical stretching of the bent structure are compared with the experimental and other theoretically derived values in table 2. In comparison to the experimental result, the energy value of the second dissociation asymptote is found to be overestimated by a small margin while values predicted by previous theoretical calculations are underestimated by the same amount.

The dipole moment value at the bent ground state equilibrium geometry is found to be 2·51 Debye (table 1). In this present work only the singlet–singlet transitions (table 3) are considered from the ground state equilibrium geometry to some low-lying excited states. The lowest energy transition taking place between X^1A_1 ($1^1A'$) and 1^1B_1 ($1^1A''$), corresponds to a transition moment value of 0·65 D. Next two transitions are having transition energies close to 20 eV. These high transition energies correspond to far UV region. As mentioned earlier, transition moments and oscillator strengths reported in this work are calculated by the GAMESS program at the ground state equilibrium geometry using the GUGA-CI wave functions.

3.2 H_2Cl^+

Table 4 shows the equilibrium geometries computed for the ground state (X^1A_1) and some low-lying excited states (1^3A_2, 1^1A_2, 1^3B_1, 1^1B_1, 1^3A_1, 1^3B_2, 2^1A_1, 1^1B_2) in the C_{2v} symmetry. Geometry obtained for the ground state almost matches with the values obtained by other experimental[26,27,29] and theoretical groups.[20,22,32,33,35,36] The ground state (X^1A_1) electronic configuration has a dominant contribution from the $4a_1^2 2b_2^2 5a_1^2 2b_1^2$ configuration (96% at equilibrium geometry) and some low contributions from $4a_1^2 5a_1^2 2b_1^2 3b_2^2$ and $4a_1^2 2b_2 5a_1 2b_1^2 3b_2 6a_1$ configurations. $4a_1$ MO (with no nodes) has the lowest energy than other valence MOs. The higher MOs involve *p* orbitals on the chlorine atom. The *p* orbitals are differently oriented with respect to the plane containing the H atoms. The H_2Cl^+ molecule lies in the *y–z* plane with the *z* axis bisects the H–Cl–H angle. The $2b_2$ MO is generated from the $3p_y$ AO while the $5a_1$ MO is generated from the $3p_z$ AO. Both of them have no nodes in the Cl–H region and therefore have binding character. Due to the presence of one node in each of them, both MOs have higher energies than the $4a_1$ MO. Molecular orbitals generated from $3p_y$ AO has lower orbital energy than that generated from the $3p_z$ AO. Some s-p mixing has occurred in the $5a_1$ and $6a_1$ MOs generated from the 3*s* and $3p_z$ AOs. $3p_x$ orbital has no net overlap with the H atoms and it gives rise to the $2b_1$ non-bonding MO, which is localized on the chlorine atom. It has higher energy than the previous MOs as it is not stabilized through the interaction with the H 1s atomic orbitals. $3b_2$ is an antibonding type MO. The barrier to linearity for the ground state is found to be very high (table 4). This barrier at the linear conformation of the X^1A_1 ground state potential surface is found to be 2·77 eV. The bent ground state correlates with a non-degenerate linear $^1\Sigma_g^+$ state with a dominating configuration of $\sigma_g^2\sigma_u^2\pi_u^4$.

In addition to the ground state mentioned above, geometries of six higher roots ($^3A_2$, $^1A_2$, $^3B_1$, $^1B_1$, $^3A_1$ and $^3B_2$ symmetries) are also studied in the C_{2v} symmetry. Two more singlet states (2^1A_1 and 1^1B_2) are reported in table 4. Optimizations of these two states are carried out from the geometry optimization of the fourth and fifth roots of the GUGA-CI

Table 2. Comparison of the dissociation asymptote energy levels arising due to the asymmetrical stretching of one H–F bond (the other bond length is fixed at 0·96 Å and bond angle is fixed at 112°).

Dissociation asymptote	ALDET-CI	Other theoretical values	Experimental
$H^+ + HF\ (^1\Sigma^+)$	0·0	0·0	0·0
$H(^2S_g) + HF^+(X^2\Pi_i)$	3·0	2·2[a]	2·6[b]

[a][16], [b][54]

Table 3. Transition moments and oscillator strengths of some electronic transitions from the ground state at the ground-state equilibrium geometry of H_2F^+.

Transition	Transition moment (Debye)	Oscillator strength (f)
$X^1A_1(^1A')$–$1^1B_1(^1A'')$	0·65	0·03
$X^1A_1(^1A')$–$2^1A_1(^1A')$	1·12	0·09
$X^1A_1(^1A')$–$1^1B_2(^1A')$	0·85	0·06

calculation using restricted Hartree–Fock SCF method which generates only the singlet states. If the two H–Cl bond distances are varied symmetrically, the first two excited electronic states are of $^3B_1$ and $^3A_2$ symmetry. For geometry determinations of these two triplet states, MCSCF calculation (for $^3B_1$ state) and GUGA CI calculation with restricted open shell Hartree–Fock SCF method (for $^3A_2$ state), have been employed along with the ALDET-CI calculations. The first excited triplet and singlet states, namely, 1^3B_1 and 1^1B_1, respectively, are actually linear ($^3\Pi_u$ and $^1\Pi_u$) while the 1^3A_2 and 1^1A_2 states are found to be bent correlating to $^3\Delta_g$ and $^1\Delta_g$ states, respectively, in the $D_{\infty h}$ symmetry. Their equilibrium bond distances are found to be very close. The first two states originate from the excitation, $2b_1^2 \rightarrow 2b_1 6a_1$ while the latter two states originate from the $2b_1^2 \rightarrow 2b_1 3b_2$ excitation. For the A_2 states, large contributions (90%) come from the $4a_1^2 5a_1^2 2b_2^2 2b_1 3b_2$ configurations while the B_1 states are dominated by $4a_1^2 2b_2^2 5a_1^2 2b_1 6a_1$ configurations correlating to $\sigma_g^2\sigma_u^2\pi_u^3\sigma_g$ configurations in their respective linear geometries. The energy corresponding to the equilibrium geometry of the $^3\Pi_u$ state is found to be lower than the minimum energy of the $^3A_2$ state. This is also true for their singlet counterparts. Existence of the $^1\Pi_u$ state as the first excited singlet state is also supported by other theoretical studies.[35–37] The 1^3B_1 and the 1^3A_1 states, correlate at linear geometry with the doubly degenerate $^3\Pi_u$ state. Similarly, the 2^1A_1 state shows the same geometry as the 1^1B_1 state at the minimum energy point with $\sigma_g^2\sigma_u^2\pi_u^3\sigma_g$ as the leading configuration in the $D_{\infty h}$ symmetry. As mentioned earlier in fluoronium ion, a similar linear/linear Renner-Teller effect couples the electronic angular momentum to the vibrational angular momentum. The fifth and sixth excited states ($^3B_2$ and $^1B_2$) are actually the remaining components of the doubly degenerate $^3\Delta_g$ and $^1\Delta_g$ linear states, respectively. A $\sigma_g^2\sigma_u^2\pi_u^3\sigma_u$ configuration correlates with the 1^1A_2 and 1^1B_2 states in C_{2v} geometry.

Conical intersections are typical for these types of molecules due to the C_{2v} symmetry. The first two sets of excited states ($1^3A_2/1^3B_1$ and $1^1A_2/1^1B_1$) are close in energy (figure 2a). Due to the different symmetries of these states, the corresponding one-dimensional potential curves are allowed to cross. This type of conical intersection between $^1A_2$ and $^1B_1$ in C_{2v} symmetry has been studied extensively in its isoelectronic H_2S molecule.[56–58] The crossing depends on the angle. The intersection point is found to be around 1·65 Å for the $1^3A_2/1^3B_1$ pair and 1·85 Å for the $1^1A_2/1^1B_1$ pair at the ground-state equilibrium angle (93·9°) during the symmetrical stretching of the two H–Cl bonds. Keeping one H–Cl bond length fixed at 1·31 Å and bond angle at 93·9°, if the other H–Cl bond distance is varied, two $^3A''$ states correspond to the 1^3A_2 and 1^3B_1 states. Similarly, two $^1A''$ states are found to correlate to the 1^1A_2 and 1^1B_1 states during the asymmetrical stretching of one H–Cl bond. The crossing of these two pair ($1^3A_2/1^3B_1$ and $1^1A_2/1^1B_1$) of states in C_{2v} symmetry changes to an avoided one in the C_s symmetry. The lower $^3A''$ state and the lower $^1A''$ state

Table 4. Spectroscopic parameters of ground state and some low-lying excited states of H_2Cl^+.

States in C_{2v} symmetry	Level of study	Equilibrium geometry		Most dominant configuration	Energy barrier to linearity (eV)	Dipole moment at equilibrium geometry (Debye)
		Bond length (H–Cl) (Å)	Bond angle (H–Cl–H) (deg)			
X^1A_1	**ALDET-CI**	1·310	93·9	$4a_1^2 2b_2^2 5a_1^2 2b_1^2$	2·77	2·07
	GUGA-CI	1·299	94·7		2·73[d]	2·14[d]
	SCF (UHF)[a]	1·286	97·0		3·01[e]	
	SCF[b]	1·290	97·3			
	MP2 (fu11)[b]	1·293	95·9			
	MP2 (full)[b]	1·300	94·2			
	CEPA-1[c]	1·303	94·2			
	MRCI[d]	1·300	94·2			
	DIM[e]	1·328	95·5			
	Exptl.[f]	1·304	94·3			
	Exptl.[g]	1·304	94·2			
	Exptl.[h]	1·320	94·2			
1^3B_1 ($^3\Pi_u$ at equilibrium)	**MCSCF**	1·580	180	$4a_1^2 2b_2^2 5a_1^2 2b_1 6a_1$	0·00	0·00
	ALDET-CI	1·563	180	($\sigma_g^2\sigma_u^2\pi_u^3\sigma_g$ at		
	SCF (UHF)[a]	1·570	180	equilibrium geometry)		
1^3A_1 ($^3\Pi_u$ at equilibrium)	**ALDET-CI**	1·563	180	$4a_1^2 2b_2^2 5a_1 2b_1^2 6a_1$ ($\sigma_g^2\sigma_u^2\pi_u^3\sigma_g$ at equilibrium geometry)	0·00	0·00
1^1B_1 ($^1\Pi_u$ at equilibrium)	**ALDET-CI**	1·603	180	$4a_1^2 2b_2^2 5a_1^2 2b_1 6a_1$	0·00	0·00
	GUGA-CI	1·613	180	($\sigma_g^2\sigma_u^2\pi_u^3\sigma_g$ at		
	MRCI[d]	1·587	180	equilibrium geometry)		
	DIM[e]	1·531	180			
2^1A_1 ($^1\Pi_u$ at equilibrium)	**ALDET-CI**	1·603	180	$4a_1^2 2b_2^2 5a_1 2b_1^2 6a_1$	0·00	0·00
	GUGA-CI	1·613	180	($\sigma_g^2\sigma_u^2\pi_u^3\sigma_g$ at		
	MRCI[d]	1·587	180	equilibrium geometry)		
1^3A_2	**ALDET-CI**	1·640	80·5	$4a_1^2 5a_1^2 2b_2^2 2b_1 3b_2$	3·50	1·51
	GUGA-CI (ROHF)	1·580	81·0			
1^1A_2	**GUGA-CI**	1·607	79·3	$4a_1^2 5a_1^2 2b_2^2 2b_1 3b_2$	4·06	1·90
1^1B_2	**GUGA-CI**	2·002	109·9	$4a_1^2 2b_2^2 5a_1 2b_1^2 3b_2$	0·35	2·78

[a][20], [b][22], [c][33], [d][35], [e][36], [f][26], [g][27], [h][29]

are found to be dissociative in nature. These states are found to dissociate into $H(^2S_g)$ and HCl^+ ($X^2\Pi_i$), while the upper A″ states ($5a'^2 6a'^2 7a'^2 2a'' 9a'$) are bound and correspond to a higher dissociation asymptote. Due to the conical intersections of the A_2 and B_1 states in the triplet and singlet symmetries, the excited molecule may leak from the upper A″ adiabatic states to the lower A″ states and dissociate. It should be noted that the conical intersection of the triplet states occur at a bond distance which is much closer to the Franck–Condon region in comparison to the intersection point of the singlet states. There is only one $^1A'$ state (figure 2c), correlating to the second dissociation asymptote, $H^+ + HCl$ ($^1\Sigma^+$). A comparison of the calculated energies of the dissociation asymptotes with the experimentally derived and theoretically predicted values are shown in table 5. The energy of the first dissociation level is found to be almost accurate with a small deviation (0·03 eV) from the experimental value. Figure 2b shows the bending potential energy curves of the above mentioned singlet and triplet states at fixed H–Cl bond length of 1·31 Å. The crossing of the 1^3A_2 and 1^3B_1 states which becomes an avoided one in the C_s symmetry is observed at 104°. Similar crossing for their singlet counterparts is found to take place at 109°.

At the equilibrium geometry of the ground state, the dipole moment value is found to be 2·07 Debye. Dipole moment values of the higher states at their

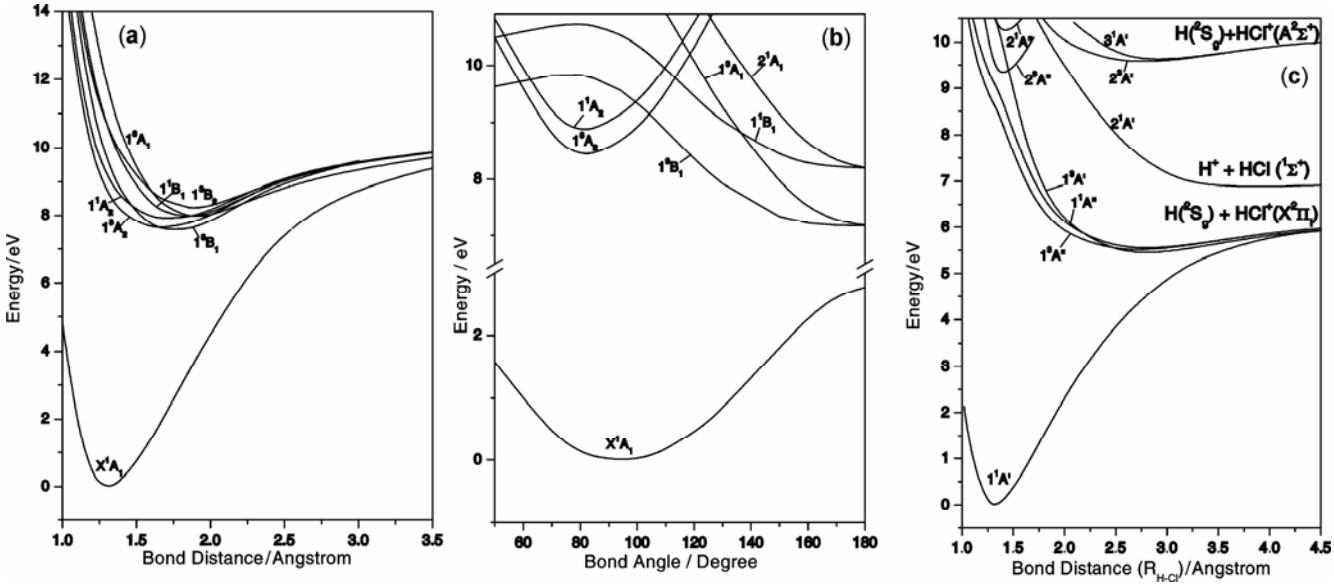

Figure 2. (**a**) One-dimensional potential energy curves of low-lying electronic states during the symmetrical stretching of H–Cl bonds at the ground-state equilibrium bond angle (93·0°). (**b**) Bending potential energy curves of the ground-state and low-lying excited states of H_2Cl^+ at R_{H-Cl} = 1·31 Å. (**c**) Potential energy curves of low-lying electronic states of H_2Cl^+ during asymmetrical stretching of one H–Cl bond (the other H–Cl bond distance is kept fixed to 1·31 Å and bond angle is fixed at 93·9°).

respective equilibrium geometries are reported in table 4. Electronic transition moments for transitions taking place from the ground state (X^1A_1) equilibrium geometry (calculated at GUGA-CI level) to the low-lying excited singlet states have been reported in this work (table 6). The high transition energies correspond to the far UV region. Transition from the ground state to the 1^1A_2 state is a forbidden one. table 6 shows that the X^1A_1 ($^1A'$)–1^1B_1 ($^1A''$) transition is the lowest energy transition with a low transition moment value. The next two transitions, X^1A_1 ($^1A'$)–1^1B_2 ($^1A'$) and X^1A_1 ($^1A'$)–2^1A_1 ($^1A'$), with approximately 15 eV transition energies have higher transition moments. Corresponding oscillator strengths of all these transitions are also reported.

In this present work, spin-orbit coupling effect has not been investigated. Spin-orbit coupling may play some role in the singlet–triplet energy separation and mixing of the states taking part in the conical intersections. The singlet–triplet gap is expected to be altered if spin-orbit effect is strong. The single group symmetry (C_{2v}) transforms to the spin double group (C_{2v}^2) after including the spin-orbit effect in the Hamiltonian. Same symmetry states in the spin double group can mix. In the C_{2v} group, $^1A_1$ corresponds to the A_1 state in the C_{2v}^2 group. Similarly, $^3B_1$ correlates to the A_2, B_2, B_1 states in the spin double group. The mixing coefficient is inversely proportional to the S_0–T_1 separation. In comparison to fluoronium ion, the heavier H_2Cl^+ is expected to show more significant spin-orbit coupling effect. The $^1A_1(A_1)$ and $^3B_1(A_1)$ states are likely to interact if the magnitude of energy separation between them is not very high. In chloronium ion, this energy gap (~8 eV) is extremely large and consequently there will be absolutely no net significant change in the singlet–triplet gap after including the spin-orbit effect. As a consequence of this, the $^1A_1(A_1)$–$^3B_1(A_1)$ transition seems to be a forbidden one even after inclusion of the spin-orbit coupling. It is possible that in bromonium and iodonium ions, this gap may be considerably influenced by the spin-orbit coupling, as this separation is expected to be much narrow in these cases. The conical intersection of the $^3A_2/^3B_1$ pair in chloronium ion is likely to be influenced by the interaction of the A_1, B_1, B_2 components of the $^3A_2$ state with their spin-orbit counterparts in the $^3B_1$ state. However, the triplet state populations will be negligibly small due to the above mentioned reason and thus the triplet state conical intersection is insignificant from the pre-dissociation point of view. The important conical intersection of the $^1A_2/^1B_1$ pair is expected to be unaffected as no spin-orbit contamination is possible for their spin double group components, $^1A_2(A_2)$ and $^1B_1(B_1)$. So the pre-dissociation seems to be governed by this intersection

Table 5. Comparison of the dissociation asymptote energy levels arising due to the asymmetrical stretching of one H–Cl bond (the other bond length is fixed at 1·31 Å and bond angle is fixed at 93·9°).

Dissociation asymptote	ALDET-CI	Other theoretical values	Experimental
$H(^2S_g) + HCl^+(X^2\Pi_i)$	–0·882	–1.22[a], –0·96[a]	–0·847[b]
$H^+ + HCl\ (^1\Sigma^+)$	0·0	0·0	0·0
$H(^2S_g) + HCl^+(A^2\Sigma^+)$	2·99	2·76[a], 2·62[a]	2·702[b]

[a][35], [b][54]

Table 6. Transition moments and oscillator strengths of some electronic transitions from the ground state at the ground-state equilibrium geometry of H_2Cl^+.

Transition	Transition moment (Debye)	Oscillator strength (f)
$X^1A_1(^1A') - 1^1B_1(^1A'')$	0·48	0·011
$X^1A_1(^1A') - 1^1B_2(^1A')$	1·07 1·21[a]	0·066
$X^1A_1(^1A') - 2^1A_1(^1A')$	1·18 1·17[a]	0·083

[a][35]

rather than the previous one. So the whole process, starting from the transition to the 1^1B_1 state in the C_{2v} symmetry and ultimately leading to the dissociation products through the repulsive $1^1A''$ state along the asymmetric stretching path via conical intersection, is likely to be unaffected by the spin-orbit coupling.

3.3 *Comparative study of the spectroscopic properties of H_2F^+ and H_2Cl^+*

The difference in the equilibrium geometry of these two ions is easily understandable from the electronegativity difference of fluorine and chlorine atoms. The higher electronegativity of fluorine atom in H_2F^+, draws the bonded electrons towards itself which opens up the bond angle and the bond distance is also shortened. The vacant d orbitals of chlorine atom in H_2Cl^+ are also responsible for its smaller bond angle. Consequently, the energy barrier to linearity of the ground state is very small (0·84 eV) in the fluoronium ion in comparison to the very high value (2·77 eV) in the chloronium ion. One major difference in their behaviour is obtained in the properties of the excited triplet and singlet states. In H_2F^+, the pair of triplet and singlet states, namely, $1^3A_2/1^3B_1$ and $1^1A_2/1^1B_1$, respectively, undergo no intersection, whereas in H_2Cl^+, conical intersection is observed for each of them. The intersection of 1^3A_2 and 1^3B_1 takes place closer to the Franck–Condon region than the intersection point of the corresponding singlet states. It has been already mentioned that these intersections in the A_2 and B_1 states imply that the excited state molecule may predissociate from the upper bound adiabatic A″ states to the lower repulsive A″ states. There is no such leakage possible for the other ion. This observation is quite similar to the behaviour of H_2O and H_2S, those are the isoelectronic species of H_2F^+ and H_2Cl^+, respectively. Considering only the singlet states, $1^1A''$ and $2^1A''$ are responsible for the photodissociation of H_2Cl^+, whereas, only the lower dissociative $^1A''$ state is responsible for the same in H_2F^+. The $X^1A_1(^1A')$–$1^1B_1(^1A'')$ transition is the lowest energy singlet–singlet transition, which is allowed both in C_{2V} and C_s symmetry. This is expected to correspond to a diffuse band in the chloronium ion in the far ultraviolet region spectrum due to the above mentioned pre-dissociation, initiated by the intersection of 1^1A_2 and 1^1B_1 states. Another low-lying singlet–singlet transition which is dipole-forbidden in the C_{2V} symmetry but allowed in the C_s symmetry, has almost negligible transition moment and oscillator strength due to the repulsive nature of $1^1A''$, in this ion. Another interesting difference is observed between these two halonium ions when one bond

length and the bond angle are kept fixed at the ground state equilibrium values and the other bond is stretched. The dissociation asymptote, $H(^2S_g)$ + HCl^+ ($X^2\Pi_i$), is found to be the lowest one in case of H_2Cl^+, while asymmetrical stretching of the lowest $^1A'$ state of H_2F^+ correlates to the first dissociation limit which produces H^+ and HF ($^1\Sigma^+$). This is due to the difference in the ionization energy values of HF and HCl. Ionization energy of HF is found to be higher than the ionization energy of H atom while for HCl molecule, it is lower than H atom. During the above mentioned stretching of one H–Cl bond in chloronium ion, a strong avoided crossing is observed between the two low–lying $^1A'$ states at 3·60 Å bond distance. Due to this strong repulsion, the $^1A'$ state, with the electronic configuration, $5a'^26a'^27a'^22a''^28a'$, corresponds to the lowest dissociation asymptote while the other $^1A'$ state with $5a'^26a'^27a'^22a''^2$ configuration correlates to the next dissociation limit. If this avoided crossing would have not been observed then the $^1A'$ state with closed shell configuration would have given different lowest energy products, H^+ + HCl ($^1\Sigma^+$), which is impossible due to the above mentioned ionization energy factor. There is no such repulsion observed in the two low-lying $^1A'$ states of fluoronium ion in the C_s symmetry, as the energy gap between them is very high in comparison to the chloronium ion.

4. Conclusion

Ab initio-based CI calculations with 6-311G (3*d*, 3*p*) basis sets have predicted the ground state and excited state geometries almost accurately. Comparative studies of electronic spectra of the two halonium ions have revealed many interesting differences in their spectroscopic properties. The intersections of the excited states during the symmetrical stretching and bending motions in H_2Cl^+ have been highlighted as the most likely reason behind the major differences in the properties of these two ions in their far ultraviolet spectroscopy. Chloronium ion becomes pre-dissociative and two excited states are found to be responsible for its photodissociation. On the other hand, molecules from the lower repulsive excited state dissociate directly in fluoronium ion. These observations are quite similar to their respective isoelectronic species except the high transition energies in these cases. It can be concluded that the major importance of this work lies in the prediction of the excited state properties of these two ions. Hopefully, this present work will motivate experimentalists to carry out more detailed studies on the far UV spectra of fluoronium and chloronium ions in the near future.

References

1. Hantzsch A 1927 *Chem. Ber.* **60** 1933
2. Hantzsch A 1928 *Z. Phys. Chem.* **134** 413
3. Couzi M, Cornut J C and Huong P V 1972 *J. Chem. Phys.* **56** 426
4. Schäfer E and Saykally R J 1984 *J. Chem. Phys.* **80** 2973
5. Schäfer E and Saykally R J 1984 *J. Chem. Phys.* **81** 4189
6. Hirota E 1988 *Phil. Trans. R. Soc. Lond.* **A324** 131
7. Swanton D J, Bacskay G B and Hush N L 1986 *Chem. Phys.* **107** 25
8. Wight G R and Brion C E 1974 *Chem. Phys. Lett.* **26** 607
9. Lischka H 1973 *Theor. Chim. Acta* **31** 39
10. Diercksen G H F, Von Niessen W and Kraemer W P 1973 *Theoret. Chim. Acta* (*Berl*) **31** 205
11. Leibovici C L 1974 *Int. J. Quantum Chem.* **8** 193
12. Wild U P, Ha T K, Raggio G A, Keller H U and Brunner P O 1975 *Helvetica Chim. Acta* **58** 696
13. Lathan W A, Hehre W J, Curtiss L A and Pople J A 1971 *J. Am. Chem. Soc.* **93** 6377
14. Pople J A and Binkley J S 1975 *Mol. Phys.* **29** 599
15. Wendell K, Jones C A, Kaufman J J and Koski W S 1975 *J. Chem. Phys.* **63** 750
16. Kendrick J, Kuntz P J and Hiller I H 1978 *J. Chem. Phys.* **68** 2373
17. Mahan B H, SchaeferIII H F and Ungemach S R 1978 *J. Chem. Phys.* **68** 781
18. Zembekov A A 1981 *Mol.Phys.* **44** 1399
19. Mavridis A and Harrison J F 1982 *J. Chem. Soc. Faraday Trans. 2* **78** 447
20. Li Y, Wang X, Jensen F, Houk K N and Olah G A 1990 *J. Am. Chem. Soc.* **112** 3922
21. Bunker P R, Jensen P, Wright J S and Hamilton I P 1990 *J.Mol. Spectrosc.* **144** 310
22. Boldyrev A and Simons J 1992 *J. Chem. Phys.* **97** 4272
23. Jura M 1974 *Astrophys. J.* **190** 33
24. Amin M Y 1996 *Earth, Moon, Planets* **73** 133
25. Blake G A, Anicich V and Huntress Jr. W T 1986 *Astrophys. J.* **300** 415
26. Kawaguchi K and Hirota E 1986 *J. Chem. Phys.* **85** 6910
27. Lee S K, Amano T, Kawaguchi K and Oldani M 1988 *J. Mol. Spectrosc.* **130** 1
28. Saito S, Yamamoto S and Kawaguchi K 1988 *J. Chem. Phys.* **88** 2281
29. Araki M, Furuya T and Saito S 2001 *J. Mol. Spectrosc.* **210** 132
30. Jorgensen W L 1978 *J. Am. Chem. Soc.* **100** 1057
31. DeFrees D J and McLean A D 1985 *J. Chem. Phys.* **82** 333

32. Botschwina P 1983 *Molecular ions: Geometric and electronic structure* (eds) J Berkowitz and K-O Groeneved (New York: Plenum) 411
33. Botschwina P 1988 *J. Chem. Soc., Faraday Trans. 2* **84** 1263
34. Curtiss L A, Raghavachari K, Trucks G W and Pople J A 1991 *J. Chem. Phys.* **94** 7221
35. Glenewinkel-Meyer Th, Ottinger Ch, Rosmus P and Werner H-J 1991 *Chem. Phys.* **152** 409
36. Kuntz P J, Roach A C and Hirst D M 1991 *J. Phys. Chem.* **95** 8364
37. Kuntz P J, Whitton N, Paidarova I and Polak R 1994 *Can. J. Chem.* **72** 939
38. Schmidt M W, Baldridge K K, Boatz J A, Elbert S T, Gordon M S, Jensen J J, Koseki S, Matsunaga N, Nguyen K A, Su S, Windus T L, Dupuis M and Montgomery J A 1993 *J. Comput. Chem.* **14** 1347
39. Ivanic J and Ruedenberg K 2001 *Theoret. Chem. Acc.* **106** 339
40. Brooks B and Schaefer H F 1979 *J. Chem. Phys.* **70** 5092
41. Brooks B, Laidig W, Saxe P, Handy N and Schaefer H F 1980 *Physica Scripta* **21** 312
42. Davidson E R 1975 *J. Comput. Phys.* **17** 87
43. Elbert S T 1987 *Theoret. Chim. Acta* **71** 169
44. Schmidt M W and Gordon M S 1998 *Ann. Rev. Phys. Chem.* **49** 233
45. Roos B O 1983 *Methods in computational molecular physics* (eds) G H F Diercksen and S Wilson (Netherlands: D. Reidel Publishing, Dordrecht)
46. Roos B O 1994 *Lecture notes in quantum chemistry* (eds) B O Roos (Berlin: Springer-Verlag), vol. 58
47. Olsen J, Yeager D L and Jorgensen P 1983 *Adv. Chem. Phys.* **54** 1
48. Werner H-J 1987 *Adv. Chem. Phys.* **69** 1
49. Shepard R 1987 *Adv. Chem. Phys.* **69** 63
50. Windus T L, Schmidt M W and Gordon M S 1994 *Theor. Chim. Acta* **89** 77
51. Weinhold F 1970 *J. Chem. Phys.* **54** 1874
52. Bauschlicher C W and Langhoff S R 1991 *Theoret. Chim. Acta* **79** 93
53. Koseki S and Gordon M S 1987 *J. Mol. Spectrosc.* **123** 392
54. Huber K P and Herzberg G 1979 *Molecular spectra and molecular structure IV: constants of diatomic molecules* (New York: Van Nostrand)
55. Lin K, Cotter R J and Koski W S 1974 *J. Chem. Phys.* **61** 905
56. Skouteris D, Hartke B and Werner H-J 2001 *J. Phys. Chem.* **A105** 2458
57. Weide K, Staemmler V and Schinke R 1990 *J. Chem. Phys.* **93** 861
58. Köppel H, Gronki J and Mahapatra S 2001 *J. Chem. Phys.* **115** 2377